

Design and motion simulation of a two-stage flapping mechanism

Chengwei Zhang, Yanjing Wu

College of Engineering, China University of Petroleum-Beijing at Karamay, Karamay City, Xinjiang Uygur Autonomous Region, China

Abstract: In order to improve the structural form and motion performance of traditional flapping aircraft, this paper designs a two-stage flapping mechanism based on the flight motion characteristics of small and medium-sized birds. In order to improve the structural form and motion performance of traditional flapping aircraft, this paper designs a two-stage flapping mechanism based on the flight motion characteristics of small and medium-sized birds. In order to improve the structural form and motion performance of traditional flapping aircraft, this paper designs a two-stage flapping mechanism based on the flight motion characteristics of small and medium-sized birds. The results show that the minimum transmission angle of the designed flapping mechanism is $\gamma_{\min}=40.26^\circ$. The flapping range of the inner wing is $\Delta\delta_1=49.27^\circ$, the upper flapping limit of the inner wing is $\delta_{\max1}=46.08^\circ$, the lower flapping limit is $\delta_{\min1}=-3.18^\circ$, the flapping range of the outer wing is $\Delta\delta_2=82.18^\circ$, the upper flapping limit of the outer wing mechanism is $\delta_{\max2}=90.94^\circ$, and the lower flapping limit is $\delta_{\min2}=8.76^\circ$.

Keywords: Two-stage bionic flapping wing mechanism, kinematics analysis, ADAMS

1. Introduction

From the perspective of bionics, flapping-wing aircraft is designed by imitating the flight mode of birds, in order to improve the flight characteristics of existing aircraft, a new type of aircraft with broad application prospects. At present, the technology of fixed-wing and rotary-wing aircraft is very complete, but their flight performance is poor at a small space scale due to the limitation of their own flight mechanism. The flapping-wing aircraft is different from traditional aircraft in the principle of generating flight lift, which makes it show the incomparable advantages of traditional aircraft at a smaller scale. Specifically, compared with traditional aircraft, flapping-wing aircraft has the advantages of high aerodynamic efficiency, good miniaturization, high control efficiency, diverse application scenarios, and flexible flight movements, making it a research hotspot at home and abroad.

Therefore, based on the single-degree-of-freedom flapping mechanism, the author designs a two-stage wing flapping mechanism by adding a second-level rod set to achieve the coupling of flapping and folding motion. In this way, the flight characteristics of birds can be better simulated, and at the same time, the problem of overly complicated flapping mechanism caused by increasing the degree of freedom is avoided.

2. Flapping mechanism design

Considering the flight characteristics of birds and ensuring that the designed flapping mechanism is relatively simple and reliable, the following restrictions are imposed on the designed flapping mechanism: 1. The degree of freedom of the designed flapping mechanism is one. 2. Simplify the flapping form of the flapping wing mechanism, so that the flapping wing only reciprocates up and down in one plane. 3. Ensure that the movement of the left and right wings is a strictly symmetrical synchronous flutter. 4. According to the flight characteristics of birds, the flapping mechanism should have the characteristics of rapid return. 5. In order to better imitate the flight characteristics of birds, the flapping wing mechanism should be a "two-section wing" type. 6. The flapping mechanism designed in this paper is mainly used for small and medium flapping aircraft, and the maximum wingspan is 800mm^[3].

In this design, a two-rod and three-pair secondary rod group is added on the basis of the double-crank and double-rocker mechanism to form the flapping mechanism to be designed. A crank-rocker mechanism is used to provide reciprocating motion when flapping. The two-rod and three-pair secondary

rod group is respectively connected to the connecting rod of the flapping mechanism and the inner wing rod through two rotating pairs. The secondary lever group cooperates with the flapping of the crank and remote lever mechanism to complete the folding action of the inner and outer wings of the mechanism, and then drives the flapping and folding motion of the wing only by the rotation of the remote lever. The overall effect diagram of the organization is shown in the figure 1.

$$F = 3n - 2P_L - P_H \tag{1}$$

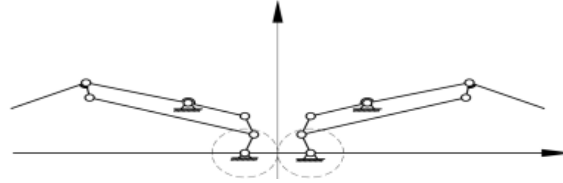


Figure 1: Schematic diagram of the flapping mechanism

In order to make the flapping mechanism have a certain motion [4], the free checking of the mechanism is carried out according to formula (1). In the formula, the number of free members $N=3$, the number of low pairs $p_l=4$, the number of high pairs $p_h=0$, and the degree of freedom of the double crank and double rocker mechanism is one. The degree of freedom of the two-rod and three-pair secondary rod group connected in series on the crank-rocker mechanism is zero. Therefore, the degree of freedom of the entire mechanism is 1, and the mechanism has a definite movement in the presence of an active member.

3. Kinematics analysis of flapping mechanism

3.1. Dimensional design of each component

Since the whole flapping mechanism is completely symmetrical with respect to the central axis, one side of the wing is selected to design the size of the mechanism rods. The motion diagram of the unilateral flapping mechanism is shown in Figure (2). First, design and calculate the size of each rod in the inner wing mechanism. Figure (3) is the principle diagram of the inner wing crank-rocker mechanism, In the figure $\delta_0 = \cos^{-1}(l/d)$, δ is the swing angle of the CD rod, that is, the swing angle of the inner wing mechanism, and a, b, and c represent the lengths of the rods AB, BC, and CD respectively, and d represents the distance between the rotating pair A and the rotating pair D.

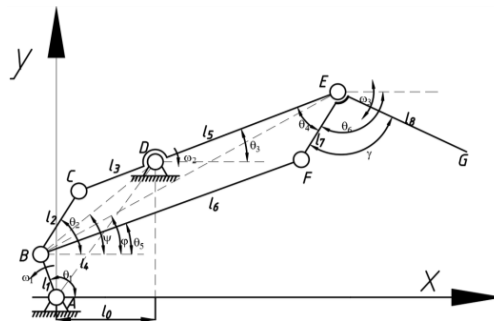


Figure 2: Simple diagram of unilateral flapping mechanism

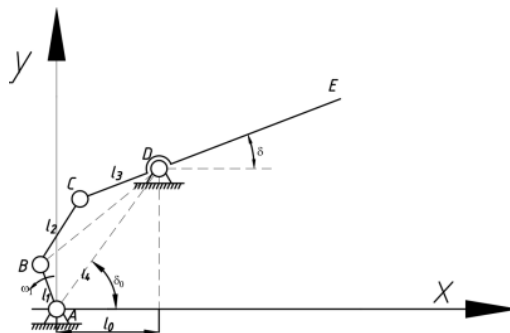


Figure 3: Schematic of the inner wing mechanism

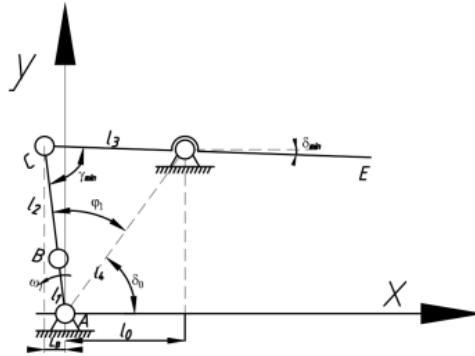


Figure 4: Lower limit position diagram of inner wing mechanism

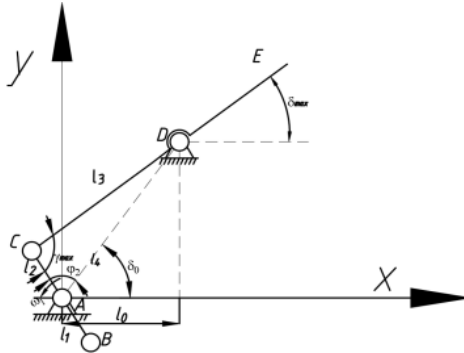


Figure 5: Inner wing mechanism upper limit position

Figures (4) and (5) show the extreme position where the rod AB and the rod CD are straightened and co-linear, and at this time γ_{max} and γ_{min} are the maximum or minimum value of the transmission angle of the mechanism in one motion cycle. δ_{max} and δ_{min} are the upstroke angle and the downstroke angle of the flapping mechanism, respectively, and the absolute value of the difference between the two angles is the swing range of the rocker. The absolute value of φ_1 and φ_2 between the two angles is the pole angle of the flapping wing mechanism. The value of LB represents the distance of the leftmost endpoint from the center plane. According to the geometric relationship, the above parameters can be calculated by formulas (2)~(5).

$$\begin{cases} \gamma_{max} = \cos^{-1} \left[\frac{(b+a)^2 + c^2 - d^2}{2 \cdot b \cdot c} \right] \\ \gamma_{min} = \cos^{-1} \left[\frac{(b-a)^2 + c^2 - d^2}{2 \cdot b \cdot c} \right] \end{cases} \quad (2)$$

$$\begin{cases} \delta_{min} = \left| \cos^{-1} \left[\frac{c^2 + d^2 - (a+b)^2}{2 \cdot c \cdot d} \right] - \delta_0 \right| \\ \delta_{max} = \left| \cos^{-1} \left[\frac{c^2 + d^2 - (b-a)^2}{2 \cdot c \cdot d} \right] - \delta_0 \right| \end{cases} \quad (3)$$

$$\begin{cases} \varphi_1 = \cos^{-1} \left[\frac{(a+b)^2 + d^2 - c^2}{2 \cdot (a+b) \cdot d} \right] \\ \varphi_2 = \cos^{-1} \left[\frac{(b-a)^2 + d^2 - c^2}{2 \cdot (b-a) \cdot d} \right] \end{cases} \quad (4)$$

$$L_B = (a+b) \cdot \sin(\delta_0 + \delta_1 - 90^\circ) \quad (5)$$

After each angle value is obtained, the pole position angle φ of the flapping mechanism, the stroke speed ratio coefficient K, and the flapping amplitude $\Delta\delta$ can be calculated according to formulas (6)~(8).

$$\Delta\delta = \delta_{max} - \delta_{min} \quad (6)$$

$$\varphi = \varphi_1 - \varphi_2 \quad (7)$$

$$K = \frac{180^\circ + \varphi}{180^\circ - \varphi} \quad (8)$$

To analogize the movement of medium-sized birds in flight, take the flapping amplitude as $\delta_{\max} = 47^\circ$, the upper flapping angle as $\delta_{\min} = -3^\circ$, and the downward flapping angle as $\gamma_{\min} = 45^\circ$. In order to ensure that the mechanism has good performance of transmitting force, the minimum transmission angle is taken as about , and the travel speed ratio coefficient is about $K=1.2$. Simultaneous formulas (2), (3), (4), (5), (6), (7), (8) are solved by using the fsolve function for solving nonlinear equations in MATLAB^[5], rounded After processing, the motion parameters of the flapping mechanism are obtained as shown in Table 1:

Table 1: Mechanism parameter values

Institutional parameters	parameter design value
crank a	12mm
connecting rod b	19mm
rocker c	29mm
distance D	31mm
Horizontal distance between racks l	16mm
rack angle	69°

The rounded data is brought into the formula to calculate a series of motion parameters of the designed flapping mechanism, as shown in Table 2:

Table 2: Mechanism kinematic parameter values

Institutional parameters	parameter design value
Upstroke limit angle δ_{\max}	46.08°
Throw down limit angle δ_{\min}	-3.18°
Flutter amplitude $\Delta\delta$	49.27°
form ratio coefficient K	1.13
Minimum drive angle γ_{\min}	40.26°

The difference from the pre-designed motion parameters is small, and the length of the inner wing is designed to meet the design requirements of the flapping mechanism. According to the overall design requirements of the flapping mechanism, the size and related angles of the outer wing rods are designed. According to the wingspan of the flapping mechanism, $B=800\text{mm}$, and the half-span length of the flapping mechanism is $B/2=400\text{mm}$. The ratio of the extension length, take the length of the inner wing rod= 112mm . The design of the four-bar mechanism is that BCEF is a parallelogram, and the relevant dimensions of each outer wing bar are calculated as follows:

Table 3: Mechanism parameter values

Institutional parameters	parameter design value
Span B	800mm
inner wing l_{CE}	112mm
Inner wing stem outreach l_{DE}	83mm
outer wing l_{EG}	288mm
Auxiliary rod l_{BF}	112mm
Auxiliary rod l_{EF}	19mm
flapping angle γ	75°

3.2. Institutional Location Analysis

A plane rectangular coordinate system is established with the position of the rotating pair connected with the crank of one side of the mechanism and the frame as the origin, and based on this, a schematic diagram of the mechanism motion is drawn as shown in Figure (6). The distances and angles required during the analysis are shown in the figure.

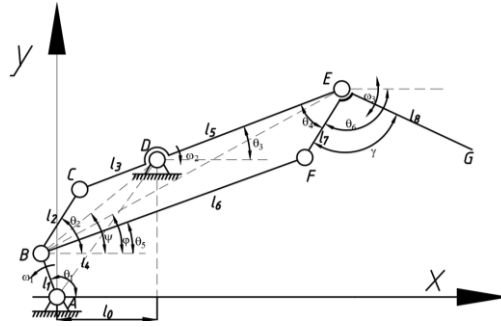


Figure 6: Sketch of unilateral flapping mechanism

Vector equations in four-rod mechanism ABCD

$$\vec{l}_1 + \vec{l}_2 = \vec{l}_3 + \vec{l}_4 \quad (9)$$

Project the vector equation to each coordinate axis and express it in coordinates to get

$$\begin{cases} x_C = x_B + l_2 \cos \theta_2 = x_D - l_3 \cos \theta_3 \\ y_C = y_B + l_2 \sin \theta_2 = y_D - l_3 \sin \theta_3 \end{cases} \quad (10)$$

Where B point coordinates can be expressed as

$$\begin{cases} x_B = l_1 \cos(\omega_1 t) \\ y_B = l_1 \sin(\omega_1 t) \end{cases} \quad (11)$$

Simultaneous formulas (9)(10)(11) can solve the unknowns θ_2 and θ_3 , in order to simplify the calculation, the equation system solution method is now transformed, and the angle is taken as

$$\psi = \arctan\left(\frac{y_D - y_B}{x_D - x_B}\right) \quad (12)$$

Then simplify θ_2 to

$$\theta_2 = \psi + \angle CBD \quad (13)$$

In $\triangle BCD$, it can be obtained from the cosine theorem

$$\angle CBD = \cos^{-1} \left[\frac{l_2^2 + (y_B - y_D)^2 + (x_B - x_D)^2 - l_3^2}{2l_2 \sqrt{(y_B - y_D)^2 + (x_B - x_D)^2}} \right] \quad (14)$$

That is, the θ_2 value can be

$$\theta_2 = \arctan\left(\frac{y_D - y_B}{x_D - x_B}\right) + \cos^{-1} \left[\frac{l_2^2 + (y_B - y_D)^2 + (x_B - x_D)^2 - l_3^2}{2l_2 \sqrt{(y_B - y_D)^2 + (x_B - x_D)^2}} \right] \quad (15)$$

At this time, the obtained θ_2 value is brought into equation (10) to get

$$\theta_3 = \sin^{-1} \left(\frac{y_D - y_B - l_2 \sin \theta_2}{l_3} \right) \quad (16)$$

At this time, the positions of point C and point E can be expressed as

$$\begin{cases} x_C = x_B + l_2 \cos \theta_2 \\ y_C = y_B + l_2 \sin \theta_2 \end{cases} \quad (17)$$

$$\begin{cases} x_E = x_C + (l_3 + l_5) \cos \theta_3 \\ y_E = y_C + (l_3 + l_5) \sin \theta_3 \end{cases} \quad (18)$$

The G point is expressed in coordinate form as

$$\begin{cases} x_G = x_E + l_8 \cos(\theta_6 - \gamma) \\ y_G = y_E - l_8 \sin(\theta_6 - \gamma) \end{cases} \quad (19)$$

where γ is a fixed value, and the unknowns in the system of equations are θ_6 , in the closed quadrilateral BCEF, the column vector equation

$$\dot{l}_2 + \dot{l}_5 = \dot{l}_3 + \dot{l}_4 + \dot{l}_6 \quad (20)$$

In the form of coordinates, we have

$$\begin{cases} x_F = x_B + l_6 \cos \theta_5 = x_C + (l_3 + l_5) \cos \theta_3 + l_7 \cos \theta_6 \\ y_F = y_B + l_6 \sin \theta_5 = y_C + (l_3 + l_5) \sin \theta_3 + l_7 \sin \theta_6 \end{cases} \quad (21)$$

There are θ_5 and θ_6 two unknowns in the formula, which θ_5 can be expressed as the difference of the two angles using the same method, namely

$$\theta_5 = \varphi - \angle EBF \quad (22)$$

In equation (21)

$$\varphi = \arctan\left(\frac{y_E - y_B}{x_E - x_B}\right) \quad (23)$$

$\angle EBF$ can be obtained from $\triangle BEF$

$$\angle EBF = \cos^{-1} \left[\frac{l_6^2 + (y_E - y_B)^2 + (x_E - x_B)^2 - l_7^2}{2l_6 \sqrt{(y_E - y_B)^2 + (x_E - x_B)^2}} \right] \quad (24)$$

θ_6 can be solved, as

$$\theta_6 = \arctan\left(\frac{y_B - y_C + l_6 \sin \theta_5 - (l_3 + l_5) \sin \theta_3}{x_B - x_C + l_6 \cos \theta_5 - (l_3 + l_5) \cos \theta_3}\right) \quad (25)$$

Put each parameter value into the above formula and use MATLAB to calculate and draw the change graph of the angular position of the inner and outer wings of the flapping mechanism with time, as shown in Figure (7).

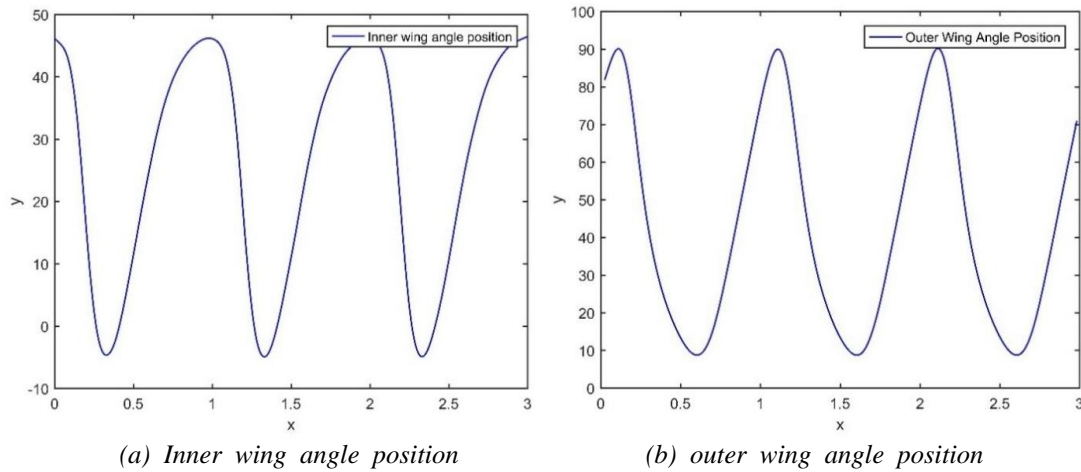


Figure 7: Inner and outer wing angle position diagram

As can be seen from Figure 7, the flapping range of the inner wing mechanism is about 50° , of which the upper flapping limit angle is about 46° , and the lower flapping limit angle is about -4° , the flapping range of the outer wing mechanism is about 83° , of which the upper throw limit angle is about 89° , and the lower throw limit angle is about 7° . In general, the angular position of the flapping mechanism of the inner and outer wings meets the design requirements of the flapping mechanism and has good motion characteristics.

3.3. Speed Analysis

The main purpose of the velocity analysis of the mechanism is to find out the velocity variation law of the inner wing rod and the outer wing rod, that is, to solve the angular velocity of the DE rod and the EG rod. To solve the swing angular velocity $\dot{\theta}_3$ of the DE rod, derivation of both sides of equation (10) can be obtained at the same time

$$\begin{cases} \dot{x}_B - l_2 \dot{\theta}_2 \sin \theta_2 = l_3 \dot{\theta}_3 \sin \theta_3 \\ \dot{y}_B + l_2 \dot{\theta}_2 \cos \theta_2 = -l_3 \dot{\theta}_3 \cos \theta_3 \end{cases} \quad (26)$$

In the formula (26)

$$\begin{cases} \dot{x}_B = -l_1\omega_1\sin(\omega_1 t) \\ \dot{y}_B = l_1\omega_1\cos(\omega_1 t) \end{cases} \quad (27)$$

Simultaneous formulas (26) and (27) can be solved

$$\begin{cases} \dot{\theta}_2 = \frac{\dot{x}_B + \dot{y}_B \tan \theta_3}{l_2(\sin \theta_2 - \cos \theta_2 \tan \theta_3)} \\ \dot{\theta}_3 = \frac{\dot{x}_B + \dot{y}_B \tan \theta_2}{l_3(\sin \theta_3 - \cos \theta_3 \tan \theta_2)} \end{cases} \quad (28)$$

Solving for the swing angular velocity of the EG rod, derivation of both sides of equation (21) can be obtained

$$\begin{cases} \dot{x}_F = \dot{x}_B - l_6\dot{\theta}_5\sin\theta_5 = \dot{x}_C - (l_3 + l_5)\dot{\theta}_3\sin\theta_3 - l_7\dot{\theta}_6\sin\theta_6 \\ \dot{y}_F = \dot{y}_B + l_6\dot{\theta}_5\cos\theta_5 = \dot{y}_C + (l_3 + l_5)\dot{\theta}_3\cos\theta_3 - l_7\dot{\theta}_6\cos\theta_6 \end{cases} \quad (29)$$

In formula (29)

$$\begin{cases} \dot{x}_C = -\omega_1 l_1 \sin(\omega_1 t) - l_2 \dot{\theta}_2 \sin \theta_2 \\ \dot{y}_C = \omega_1 l_1 \cos(\omega_1 t) - l_2 \dot{\theta}_2 \cos \theta_2 \end{cases} \quad (30)$$

In order to make the calculation result concise, here we set

$$\begin{cases} A = \dot{x}_B - \dot{x}_C + (l_3 + l_5)\dot{\theta}_3\sin\theta_3 \\ B = \dot{y}_B - \dot{y}_C - (l_3 + l_5)\dot{\theta}_3\cos\theta_3 \end{cases} \quad (31)$$

Simultaneously (29)(30)(31) can be solved

$$\begin{cases} \dot{\theta}_5 = \frac{A + B \tan \theta_6}{l_6(\sin \theta_5 - \cos \theta_5 \tan \theta_6)} \\ \dot{\theta}_6 = \frac{A + B \tan \theta_5}{l_7(-\sin \theta_6 + \cos \theta_6 \tan \theta_5)} \end{cases} \quad (32)$$

The relevant parameters are put into the above formulas, and MATLAB is used to calculate and draw the change graph of the speed of the inner and outer wings of the flapping mechanism with time, as shown in Figure 8.

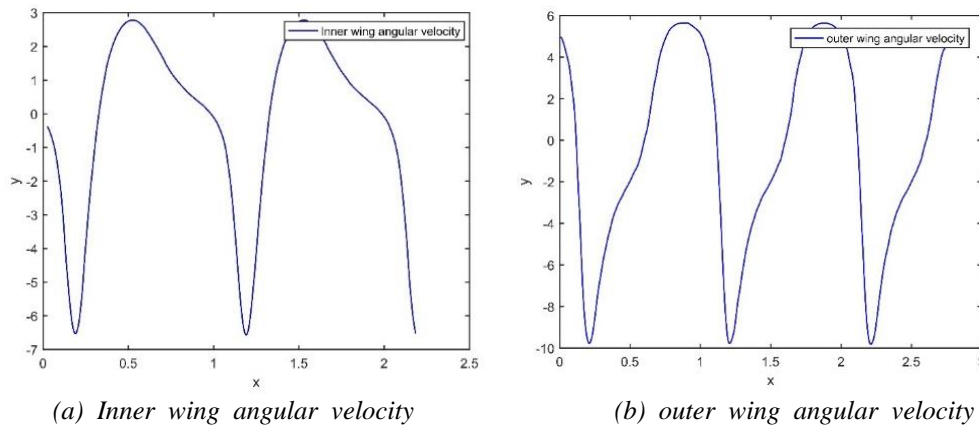


Figure 8: Inner and outer wing angular velocity diagram

It can be seen from the figure that the maximum flapping speed of the inner wing of the flapping mechanism is about 6.5rad/s during the flapping process, and the maximum flapping speed of the outer wing during the flapping process is about 9.8rad/s. In general, it can be seen from the figure that the velocity curves of the inner and outer wings of the mechanism are relatively smooth as a whole without sharp points, indicating that the movement of the inner and outer wings of the mechanism is relatively stable.

3.4. Acceleration Analysis

The purpose of the acceleration analysis is to find the relationship between the motion acceleration of the inner and outer wing rods and the angular position, the angular acceleration of the DE rod and the EG rod, first solve the angular acceleration of the DE rod, and derive both sides of the equation system

(26) at the same time.

$$\begin{cases} \ddot{x}_B - l_2 \ddot{\theta}_2 \sin \theta_2 - l_2 \dot{\theta}_2^2 \cos \theta_2 = l_3 \ddot{\theta}_3 \sin \theta_3 + l_3 \dot{\theta}_3^2 \cos \theta_3 \\ \ddot{y}_B + l_2 \ddot{\theta}_2 \cos \theta_2 - l_2 \dot{\theta}_2^2 \sin \theta_2 = -l_3 \ddot{\theta}_3 \cos \theta_3 + l_3 \dot{\theta}_3^2 \sin \theta_3 \end{cases} \quad (33)$$

in

$$\begin{cases} \ddot{x}_B = -\omega_1^2 l_1 \cos(\omega_1 t) \\ \ddot{y}_B = -\omega_1^2 l_1 \sin(\omega_1 t) \end{cases} \quad (34)$$

In order to make the calculation results more concise, here we set

$$\begin{cases} C = \ddot{x}_B - l_2 \dot{\theta}_2^2 \cos \theta_2 - l_3 \dot{\theta}_3^2 \cos \theta_3 \\ D = \ddot{y}_B - l_2 \dot{\theta}_2^2 \sin \theta_2 - l_3 \dot{\theta}_3^2 \sin \theta_3 \end{cases} \quad (35)$$

Simultaneous formulas (32) (33) (34) are solved

$$\begin{cases} \ddot{\theta}_2 = \frac{C + D \tan \theta_3}{l_2 (\sin \theta_2 - \cos \theta_2 \tan \theta_3)} \\ \ddot{\theta}_3 = \frac{C + D \tan \theta_2}{l_3 (\sin \theta_3 - \cos \theta_3 \tan \theta_2)} \end{cases} \quad (36)$$

Solving for the angular acceleration of the EG rod, taking the derivatives of both sides of the equation (29) at the same time, we can get

$$\begin{cases} \ddot{x}_B - l_6 \ddot{\theta}_5 \sin \theta_5 - l_6 \dot{\theta}_5^2 \cos \theta_5 = \ddot{x}_C - l_{CE} \ddot{\theta}_3 \sin \theta_3 - l_{CE} \dot{\theta}_3^2 \cos \theta_3 - l_{EF} \ddot{\theta}_6 \sin \theta_6 - l_{EF} \dot{\theta}_6^2 \cos \theta_6 \\ \ddot{y}_B - l_6 \ddot{\theta}_5 \cos \theta_5 - l_6 \dot{\theta}_5^2 \sin \theta_5 = \ddot{y}_C + l_{CE} \ddot{\theta}_3 \cos \theta_3 - l_{CE} \dot{\theta}_3^2 \sin \theta_3 - l_{EF} \ddot{\theta}_6 \cos \theta_6 - l_{EF} \dot{\theta}_6^2 \sin \theta_6 \end{cases} \quad (37)$$

in

$$\begin{cases} \ddot{x}_C = \ddot{x}_B - l_2 \ddot{\theta}_2 \sin \theta_2 - l_2 \dot{\theta}_2^2 \cos \theta_2 \\ \ddot{y}_C = \ddot{y}_B - l_2 \ddot{\theta}_2 \cos \theta_2 - l_2 \dot{\theta}_2^2 \sin \theta_2 \end{cases} \quad (38)$$

In order to make the calculation results more concise, here we set

$$\begin{cases} E = \ddot{x}_B - \ddot{x}_C + l_{CE} \ddot{\theta}_3 \sin \theta_3 + l_{CE} \dot{\theta}_3^2 \cos \theta_3 - l_6 \dot{\theta}_5^2 \cos \theta_5 + l_7 \dot{\theta}_6^2 \cos \theta_6 \\ F = \ddot{y}_B - \ddot{y}_C - l_{CE} \ddot{\theta}_3 \cos \theta_3 + l_{CE} \dot{\theta}_3^2 \sin \theta_3 - l_6 \dot{\theta}_5^2 \sin \theta_5 - l_7 \dot{\theta}_6^2 \sin \theta_6 \end{cases} \quad (39)$$

Simultaneously (37) (38) (39) three equations are solved

$$\begin{cases} \ddot{\theta}_5 = \frac{E + F \tan \theta_6}{l_6 (\sin \theta_5 - \cos \theta_5 \tan \theta_6)} \\ \ddot{\theta}_6 = \frac{E + F \tan \theta_5}{l_7 (\sin \theta_6 + \cos \theta_6 \tan \theta_5)} \end{cases} \quad (40)$$

Bring the relevant parameters into the above formulas and use MATLAB to calculate and draw the change graph of the acceleration of the inner and outer wings of the flapping mechanism with time, as shown in Figure 9.

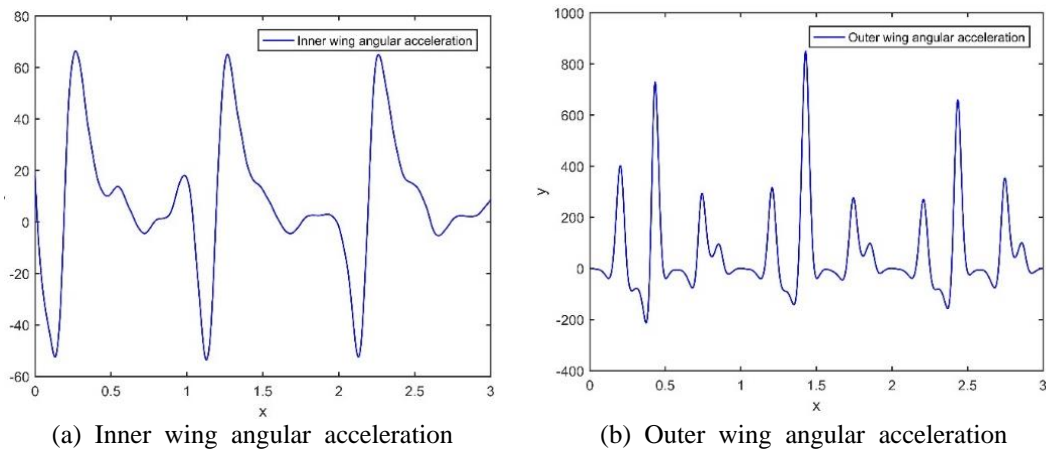


Figure 9: Inner and outer wing angular acceleration

It can be seen from the figure that the acceleration of the inner wing of the flapping mechanism has multiple extreme values in a flutter cycle, and the maximum acceleration velocity is about 70rad/s^2 ; the acceleration of the outer wing has multiple extreme values in a flutter cycle. Extreme value, where the maximum flutter speed is around 850rad/s^2 .

4. Kinematics simulation of flapping mechanism

In order to verify the correctness of the kinematic analysis in Section 3, this section uses ADAMS software to simulate and analyze the flapping wing mechanism. According to the relevant dimensions of the inner and outer wings of the flapping mechanism, the corresponding three-dimensional model is established in the SolidWorks software, and the built model is imported into the ADAMS software, and the ADAMS simulation model is obtained as shown in Figure 10.

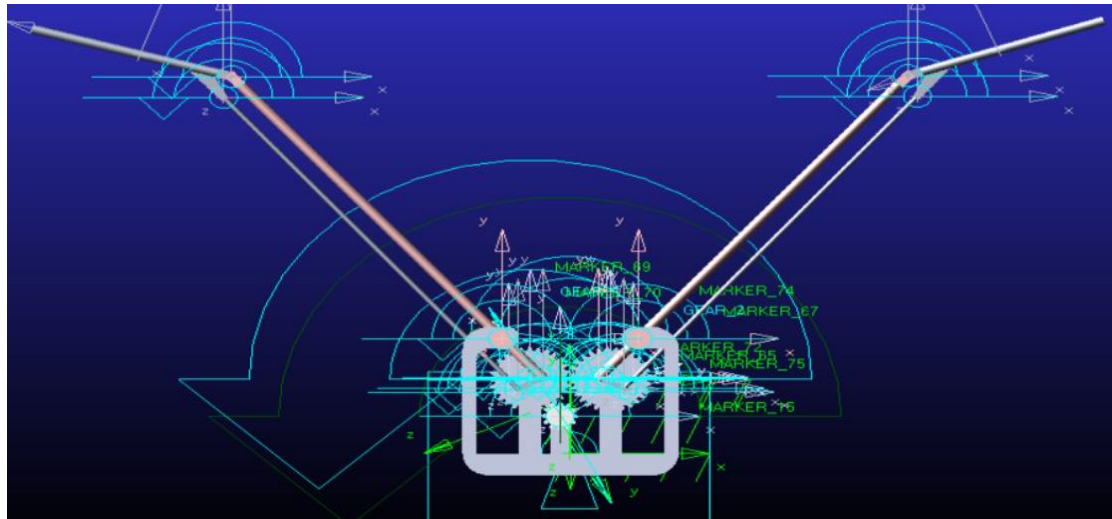
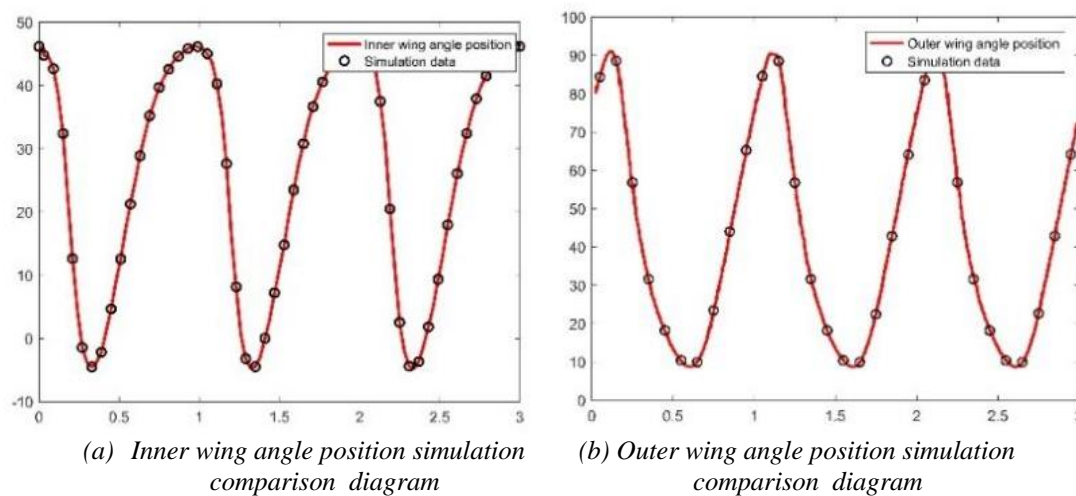


Figure 10: Simulation diagram of flapping mechanism

According to the design requirements, set the part material and add the kinematic pair and driving force at the corresponding position. Take the flapping frequency of the flapping mechanism as 4 Hz, and the given pinion speed is 1460r/min . After the gear is decelerated, the crank rotation speed is $2\pi\text{ rad/s}$. ADAMS simulation was carried out to obtain 6 sets of data of kinematic parameter changes of the inner and outer wings of the mechanism during the simulation operation, and compared with the theoretical calculation values. The comparison curves of the kinematic parameters of the inner wing and the outer wing in two cycles are shown in Figure 10



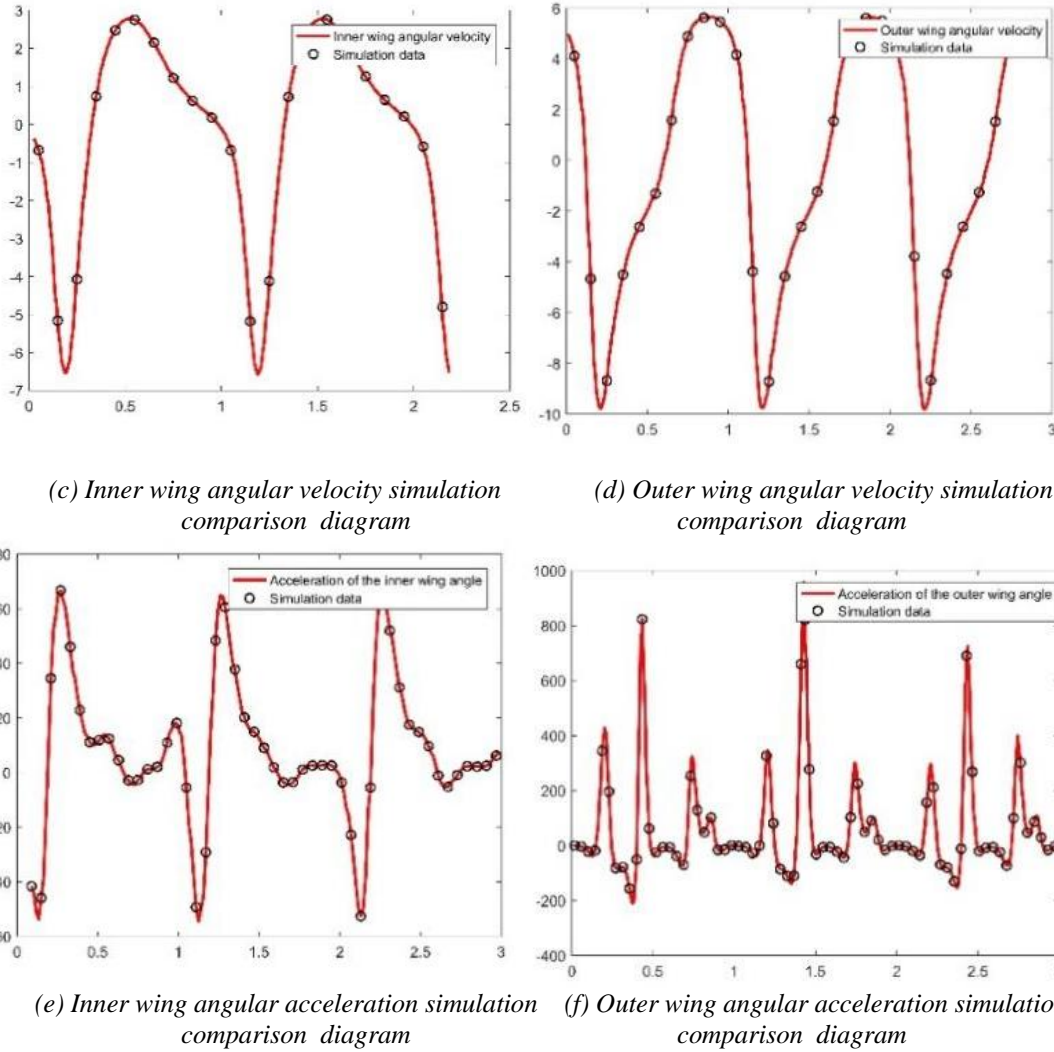


Figure 11: Comparison of theoretical calculation and ADAMS simulation output parameters

It can be seen from Fig. 11 that the variation curve of the motion parameters of the flapping wing mechanism obtained by ADAMS simulation with time is basically consistent with the calculation result of the kinematic analysis, which well proves the correctness and feasibility of the kinematic analysis.

5. Conclusion

This paper combines the flapping law of wings of medium-sized birds in flight, and is based on the traditional double-crank and double-rocker flapping mechanism. A new two-stage foldable bionic flapping wing mechanism is designed. And the kinematic and dynamic flight was carried out, and the following conclusions were obtained:

(1) During the flapping process of the flapping wing mechanism, the upper flapping limit is $\delta_{max1} = 40.26^\circ$; the lower flapping limit $\delta_{min1} = -3.18^\circ$, and the flapping amplitude of the outer wing $\Delta \delta_2 = 49.27^\circ$. The upper flapping limit of the outer wing mechanism is $\delta_{max2} = 90.94^\circ$; The lower flapping limit is $\delta_{min2} = -8.76^\circ$, which is similar to the flight motion parameters of medium-sized birds.

(2) The minimum transmission angle of the flapping wing mechanism during the flapping process is the minimum transmission angle $\gamma_{min} = 40.08^\circ$, which has good force transmission performance.

(3) Using the ADAMS flapping drive mechanism for simulation analysis, the ADAMS simulation analysis curve of the output angle of the drive mechanism is consistent with the MATLAB theoretical calculation and analysis curve, which verifies the correctness of the theoretical analysis.

References

- [1] Xie Youzeng. *Structural design and aerodynamic analysis of a bionic bird repelling flapper [D]*. Civil Aviation University of China, 2015.
- [2] Zhong Yaopeng, Wu Jilin, Lin Zhishan, Zhang Jiayu. *Design of a two-stage flapping-wing bionic aircraft [J]*. *Electromechanical Engineering Technology*, 2021, 50(S1): 9-12.
- [3] Wu Bin. *Design and analysis of active folding and deforming flapping-wing aircraft [D]*. Beijing Jiaotong University, 2019. DOI: 10.26944/d.cnki.gbjfu.2019.000190.
- [4] Shyy W, Berg M, Ljungqvist D. *Flapping and flexible wings for biological and micro air vehicles [J]*. *Progress in Aerospace Sciences*, 1999.
- [5] Jiang Hongli. *Structural design and simulation analysis of two-stage flapping-wing aircraft [D]*. Harbin Institute of Technology, 2017.
- [6] Wu Rui. *Prototype design and experimental research of a two-stage flexible bird-like flapping-wing aircraft [D]*. Harbin Institute of Technology, 2019.